2018 26th Mediterranean Conference on Control and Automation (MED)
Zadar, Croatia, June 19-22, 2018

Collaborative Visual Area Coverage by Aerial Agents under Positioning Uncertainty

Mariliza Tzes[1], Sotiris Papatheodorou[2] and Anthony Tzes[2]

Abstract— **In this article a control scheme for the coverage of a convex region by a team of Mobile Aerial Agents (MAAs) is presented. Each MAA is outfitted with a downwards facing camera, the sensed area of which is dependent on the MAA's altitude. Additionally, the MAAs' footprints are assumed to be known with a certain degree of uncertainty. In order to take into account the MAAs' positioning uncertainty as well as their varying sensed areas, an Additively Weighted Guaranteed Voronoi (AWGV) partitioning of the region is utilized. Based on this partitioning scheme, a gradient–based algorithm is derived in order to guarantee monotonic increase of an area coverage metric, while also constraining the MAAs' altitudes and it is extended to offer collision avoidance. The proposed scheme is evaluated through simulation studies.**

Index Terms— **Cooperative Control, Robotic Camera Networks, Distributed Robot Systems, Area Coverage**

I. Introduction

Distributed coverage control by multi–agent robotic systems have gained remarkable attention in recent years. Their popularity can be attributed to the technological advances in localization and communication systems, as well as the development of capable mobile robots with powerful on–board computers.

In the area coverage problem [1] a swarm of mobile, ground or aerial robots, equipped with sensors appropriate for the particular coverage application, are requested to cover a given region. Several approaches considering coverage problems have been introduced including game–theoretic methods [2], [3] or more classical methods like distributed optimization [4]and optimal control [5]. Other novel methods include event–triggered control[6] and model predictive control [7]. For coverage problems, a variety of factors should be taken into consideration. For instance, the properties and geometry of the region to be covered [8], [9], the communication capabilities of the agents [10], [11] as well as their sensor performance and type [12], [13], [14]. Another factor that should be taken into account would be the type of agents employed to achieve coverage over a region. Mobile ground vehicles or aerial vehicles [15], [16] are some of the possible choices, with particular interest often given in the vehicles' dynamics [17].

Although many works assume precise positioning of the mobile agents, in practise this is not the case. All positioning systems have an inherent uncertainty in their measurements resulting in positioning errors. There have been efforts to account for this uncertainty through methods such as data fusion from multiple localization systems [18], probabilistic models [19] or trajectory planning with safety guarantees [20]. Methods for area coverage by ground vehicles under positioning uncertainty have been proposed in the past [21] but the results have not been extended to aerial agents yet.

This article examines the coverage problem of a convex region by a team of Mobile Aerial Agents (MAAs). Each agent is equipped with a downward facing camera with a conical field of view. It is assumed that the positioning of the agents is not precise with regards to their x-y position, while their height is measured precisely. We propose the Additively Weighted Guaranteed Voronoi diagram (AWGV), instead of Guaranteed Voronoi presented in [21], in order to assign regions of interest to the agents while taking into account their positioning uncertainty and the heterogeneity of their sensing disks, resulting from their different heights.

A control law is derived in order to guarantee monotonic increase of a joint coverage–quality objective and it is extended to prevent collisions between the agents. Finally, simulations are provided in order to evaluate the performance and highlight the characteristics of the proposed control law.

The layout of the article is as follows. In Section II some mathematical preliminaries are presented. The Additively Weighted Guaranteed Voronoi diagram is presented in Section III. Section IV contains the definition of the coverage–quality objective alongside with the derivation of the proposed gradient–based control law. An extension to the derived control law for collision avoidance between the agents is also examined the same section. Finally, in Section V simulation studies are presented in order to evaluate the proposed control law and are followed by some concluding remarks.

II. Mathematical Preliminaries

Let $\Omega \in \mathbb{R}^2$ be a compact, convex, region of interest to be covered by a team of MAAs (agents). The space density function $\phi : \Omega \to \mathbb{R}_+$ expresses any a priori knowledge regarding the importance of each point $q \in \Omega$. We assume a team of n MAAs, each located at the coordinates $X_i = [x_i, y_i, z_i]^T$, $i \in I_n$ where $I_n = \{1, 2, ...n\}$. In order to simplify notation, we define $q_i \stackrel{\triangle}{=} [x_i, y_i]^T \in \Omega$ to denote agent i's projection on the region Ω. Additionally, we define the minimum and maximum operational altitudes for each MAA as $0 < z_i^{\min} < z_i^{\max}$ with $z_i \in \left[z_i^{\min}, z_i^{\max}\right]$.

Instead of a realistic kinodynamic model, such as the quadcopter model used in [22], each agent is approximated

[1] The author is with the Department of Electrical & Computer Engineering, University of Patras, Rio 26500, Greece

[2] The authors are with New York University Abu Dhabi, Engineering Division, P.O. 129188, Abu Dhabi, United Arab Emirates. Corresponding author's email: anthony.tzes@nyu.edu

by a point mass and follows the simplified kinodynamic model

$$\dot{q}_i = u_{i,q}, \quad q_i \in \Omega,\ u_{i,q} \in \mathbb{R}^2, \tag{1}$$

$$\dot{z}_i = u_{i,z}, \quad z_i \in \left[z^{min}, z^{max}\right],\ u_{i,z} \in \mathbb{R}, \tag{2}$$

where $u_{i,q}$ and $u_{i,z}$ correspond to the footprint and altitude control inputs respectively. The minimum altitude constraint $z_i^{\min}$ is used to guarantee the MAAs will not collide with ground obstacles, while the maximum altitude constraint $z_i^{\max}$ ensures they remain within range of their base station. For the sake of simplicity, in the sequel it is assumed that all MAAs have common minimum and maximum altitude constraints $z^{\min}$ and $z^{\max}$ but the results can be extended trivially to take into account differing altitude constraints among agents.

Each agent is assumed to have a measure of uncertainty with respect to its position's projection on the plane, i.e. q_i is not known precisely, while z_i is assumed to be measured accurately. By assuming that there is an upper bound r_i for the positioning uncertainty of each agent, we can define a positioning uncertainty region for each agent i

$$C_i^u(q_i, r_i) = \{q \in \Omega:\ \| q - q_i \| \leq r_i\}, \tag{3}$$

which is a disk containing all possible positions of the agent's projection on Ω given its reported position q_i and the positioning uncertainty bound r_i.

All MAAs are equipped with identical, downwards facing visual sensors with a conical field of view. This results in each MAA covering a circular region on the ground as follows

$$C_i^s(X_i, a) = \{q \in \Omega:\ \| q - q_i \| \leq z_i \tan a\}, \tag{4}$$

where a is half the angle of the visual sensor's field of view. It follows from (4) that as the altitude of an MAA increases, the radius of its sensed region C_i^s also increases.

Given the fact that each MAA may be located anywhere within its positioning uncertainty region C_i^u, we can define the guaranteed sensed region for agent i as the region on the ground that agent i is guaranteed to sense for all of its possible positions within C_i^u. Since both C_i^u and C_i^s are circular disks, the guaranteed sensed region C_i^{gs} can be written as

$$C_i^{gs}(X_i, r_i, a) = \left\{q \in \Omega:\ \| q - q_i \| \leq R_i^g(z_i)\right\}. \tag{5}$$

where $R_i^g(z_i) = z_i \tan a - r_i$. An illustration of the described visual area coverage concept can be seen in Figure 1, where the MAAs' positions are shown as red dots, their positioning uncertainty regions as black disks, their guaranteed sensed regions as grey disks and the boundaries of their sensed regions as blue circles.

Due to the nature of visual sensors, objects further away from the sensor appear with lower quality than objects near the sensor. Consequently, when an agent is at a lower altitude, it should cover a smaller area but with higher quality. In order to model this property we define the coverage quality

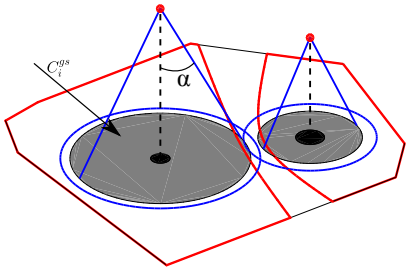

Fig. 1: MAA visual coverage concept.

function $f(z_i)\colon \left[z^{\min}, z^{\max}\right] \to [0,1]$ which is selected to be the following polynomial function

$$f(z_i) = \begin{cases} \dfrac{\left(\left(z_i - z^{\min}\right)^2 - \left(z^{\max} - z^{\min}\right)^2\right)^2}{\left(z^{\max} - z^{\min}\right)^4}, & q \in C_i \\ 0, & q \notin C_i \end{cases} \tag{6}$$

The most notable properties of $f(z_i)$ are the fact that it is a decreasing function of z_i with $f(z^{min}) = 1$ and $f(z^{max}) = 0$ and is differentiable with respect to z_i. It is emphasized that this particular selection for the coverage quality function is arbitrary and any function having the aforementioned properties could have been used instead.

III. Space Partitioning

The common practice when considering coverage problems is assigning specific regions of responsibility to each agent. Many partitioning methods have been proposed, though the most prevailing one is the Voronoi diagram. However, in the case where the agents have uncertain positioning the classic Voronoi diagram fails to take into account this positioning uncertainty. This problem is addressed by the Guaranteed Voronoi (GV) diagram [23] but the GV diagram does not account for heterogeneity in the agents' sensing patterns. In order to consider the agents' differing sensed regions due to their differing altitudes, the Additively Weighted Guaranteed Voronoi diagram (AWGV) is employed. The AWGV is an extension of the GV diagram as described in the following sections and is used to assign regions of responsibility to each agent.

A. Guaranteed Voronoi

Consider a set of uncertain regions $C^u = \{C_1^u, ..., C_n^u\}$ inside a planar region Ω, where each region C_i^u contains all possible positions of point $p_i \in C_i^u$. The Guaranteed Voronoi diagram of a set of uncertain regions results in the assignment of a cell V_i to each uncertain region as follows

$$V_i = \{q \in \Omega:\ \max \| q - p_i \| \leq \min \| q - p_j \| \\ \forall j \in I_n,\ j \neq i,\ p_i \in C_i^u,\ p_j \in C_j^u\},\ i \in I_n.$$

Each resulting cell V_i contains all the points that are guaranteed to be closer to agent i for all of the possible configurations of the agents. This is the partitioning method used in [21].

B. Additively Weighted Guaranteed Voronoi

The GV diagram can be extended by incorporating additive weights for each uncertain region, creating the Additively Weighted Guaranteed Voronoi diagram. Since the agents are heterogeneous with respect to their sensing performance, we weight each positioning uncertainty region C_i^u with the agent's guaranteed sensing radius R_i^g. This way, agents with greater sensing capabilities are assigned larger cells. The AWGV diagram for a set of uncertain regions $C^u = \{C_1^u, ..., C_n^u\},\ C_i \subset \Omega$ with weights $R^g = \{R_1^g, ...R_n^g\},\ R_i^g \in \mathbb{R}$ is defined as

$$W_i = \Big\{ q \in \Omega : \max \parallel q - p_i \parallel - R_i^g \leq \min \parallel q - p_j \parallel - R_j^g \quad \forall j \in I_n,\ j \neq i,\ p_i \in C_i^u,\ p_j \in C_j^u \Big\},\ i \in I_n. \tag{7}$$

Each cell W_i contains all the points $q \in \Omega$ which are guaranteed to be closest to agent i while taking into account its weight R_i^g for every possible position of all the agents inside their respective positioning uncertainty regions. When the weights R_i^g of all the agents are equal, the AWGV coincides with the GV. If it also holds that the agents' positioning is precise, i.e. the positioning uncertainty regions degenerate into points, then the AWGV diagram converges to the classic Voronoi diagram.

Remark 1: Similarly to the GV diagram, the AWGV diagram does not result in a complete tessellation of Ω, since a subset $\mathbb{O}$ of Ω remains unassigned. This subset contains the points that are not guaranteed to be closer to any particular agent and is called the neutral region. The neutral region is given by

$$\mathbb{O} = \Omega \setminus \bigcup_{i \in I_n} W_i.$$

Given the fact that the positioning uncertainty regions are disks, expression (7) can be further simplified into

$$W_i = \Big\{ q \in \Omega :\ \parallel q - q_i \parallel + r_i - R_i^g \leq \parallel q - q_j \parallel - r_j - R_j^g, \quad \forall j \in I_n,\ i \neq j \Big\},\ i \in I_n \tag{8}$$

which is equivalent to

$$W_i = \bigcup_{j \in I_n} H_{ij},\ i \in I_n \tag{9}$$

where

$$H_{ij} = \Big\{ q \in \Omega :\ \parallel q - q_j \parallel - \parallel q - q_i \parallel \geq r_i + r_j - R_i^g + R_j^g \Big\}.$$

The locus of the boundary ∂H_{ij} of H_{ij} is a branch of a hyperbola with foci located at points q_i and q_j and semi-major axis $2a_i = r_i + r_j - R_i^g + R_j^g$, with positive a_i corresponding to the West branch, while negative a_i to the East branch of the hyperbola. Taking this into account, $a_i > 0$ results in the region H_{ij} being convex while $a_i < 0$ results in H_{ij} being non-convex.

Remark 2: The set of neighbors N_i of agent i with respect to the Additively Weighted Guaranteed Voronoi diagram is defined as the agents with which i must communicate with in order to construct its own cell as well as provide them enough information to construct their own cells as wll. These are defined as

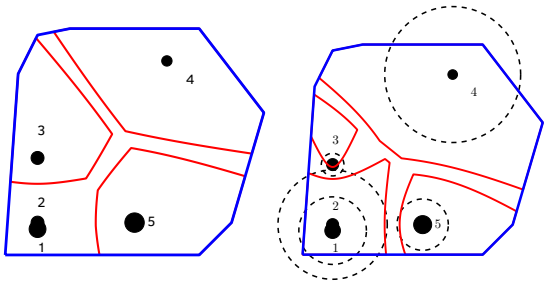

Fig. 2: Examples of the Guaranteed Voronoi (a) and Additively Weighted Guaranteed Voronoi (b) diagrams.

$$N_i = \big\{ j \in I_n \setminus i :\ \partial H_{ij} \cap W_i \neq \emptyset \vee \partial H_{ji} \cap W_j \neq \emptyset \big\}, \tag{10}$$

and consequently the cell of agent W_i can be computed as

$$W_i = \bigcup_{j \in N_i} H_{ij}.$$

In the GV diagram if two or more overlapping positioning uncertainty regions the cells of the respective agents are empty. In the AWGV diagram however, when two or more uncertainty regions overlap, the agent with the greatest weight will be assigned a non-empty cell. Figure 2 shows a comparison of the GV and AWGV diagrams for five agents, where the agents' positioning uncertainty regions are filled in black, the boundaries of their cells in red and the boundaries of their guaranteed sensed regions in dashed black lines.

IV. Distributed Control Scheme

We define the following coverage–quality objective

$$\mathscr{H} = \sum_{i \in I_n} \int_{W_i \cap C_i^{gs}} f(z_i) \phi(q)\ dq, \tag{11}$$

which expresses the area that is guaranteed to both be covered by each agent and be closer to that particular agent than any other, while also taking into account the coverage quality of each agent.

Theorem 1: In a network of MAAs, with the kinodynamic model described in (1,2), uncertain localization as specified in (3), sensing performance as in (4) and the AWGV space partitioning presented in Section III, the control law

$$u_{i,q} = \alpha_q \int_{\partial W_i \cap \partial C_i^{gs}} f(z_i) n_i \phi dq + \alpha_q \sum_{j \in N_i} \left[\int_{\partial W_i \cap \partial H_{ij}} f(z_i) v_i^i n_i \phi dq + \int_{\partial W_j \cap \partial H_{ji}} f(z_j) v_j^i n_i \phi dq \right] \tag{12}$$

$$u_{i,z} = \alpha_z \int_{\partial W_i \cap \partial C_i^{gs}} f(z_i) \tan(a) \phi dq + \int_{W_i \cap C_i^{gs}} \frac{\partial f(z_i)}{\partial z_i} dq + \alpha_z \sum_{j \in N_i} \left[\int_{\partial W_i \cap \partial H_{ij}} f(z_i) v_i^i n_i \phi dq + \int_{\partial W_j \cap \partial H_{ji}} f(z_j) v_j^i n_i \phi dq \right] \tag{13}$$

where α_q, α_z are positive constants, n_i the outward pointing unit normal vector on W_i and v_j^i and v_j^i are the Jacobian matrices of points $q \in \partial W_j$ with respect to q_i and z_i respectively, maximizes the coverage objective (11) monotonically along the agents' trajectories, leading them to a locally optimal configuration.

Proof: Since the goal is for $\mathscr{H}$ to increase in a monotonic manner, its time derivative is evaluated as

$$\frac{\partial \mathscr{H}}{dt} = \sum_{i \in I_n} \left[\frac{\partial \mathscr{H}}{\partial q_i} \dot{q}_i + \frac{\partial \mathscr{H}}{\partial z_i} \dot{z}_i \right] = \sum_{i \in I_n} \left[\frac{\partial \mathscr{H}}{\partial q_i} u_{i,q} + \frac{\partial \mathscr{H}}{\partial z_i} u_{i,z} \right]$$

By selecting the following control inputs

$$u_{i,q} = \alpha_q \frac{\partial \mathscr{H}}{\partial q_i}, \quad u_{i,z} = \alpha_z \frac{\partial \mathscr{H}}{\partial z_i}$$

we guarantee that the first derivative of $\mathscr{H}$ is non-negative thus ensuring monotonic increase of the objective.

The partial derivative $\frac{\partial \mathscr{H}}{\partial q_i}$ is computed using the Leibniz integral rule as

$$\frac{\partial \mathscr{H}}{\partial q_i} = \int_{\partial (W_i \cap C_i^{gs})} f(z_i) u_i^i n_i \phi dq + \int_{W_i \cap C_i^{gs}} \frac{\partial f(z_i)}{\partial q_i} \phi dq + \sum_{j \in I_n} \int_{\partial (W_j \cap C_j^{gs})} f(z_j) u_j^i n_i \phi dq$$

where n_j is the outward unit normal vector on $W_i \cap C_i^{gs}$ and v_j^i the Jacobian matrix

$$v_j^i = \frac{\partial q}{\partial q_i}, \; q \in \partial (W_i \cap C_i^{gs}), \; i, j \in I_n.$$

Considering the fact that $\frac{\partial f(z_i)}{\partial q_i} = 0$ and only the neighbors of agent i are affected by its motion, the second integral is equal to zero and the sum is computed over the neighbours N_i. In order to simplify the computation of the partial derivative, we use the decomposition into disjoint sets

$$\partial (W_i \cap C_i^{gs}) = \{\partial W_i \cap \partial \Omega\} \cup \{\partial W_i \cap \partial C_i^{gs}\} \cup \{\partial W_i \cap \partial \mathbb{O}\}. \quad (14)$$

These sets correspond to the parts of ∂W_i on the region boundary, on the agent's guaranteed sensed region boundary and on the boundary of the neutral region which are shown in Figure 3 in solid blue, green and red lines respectively.

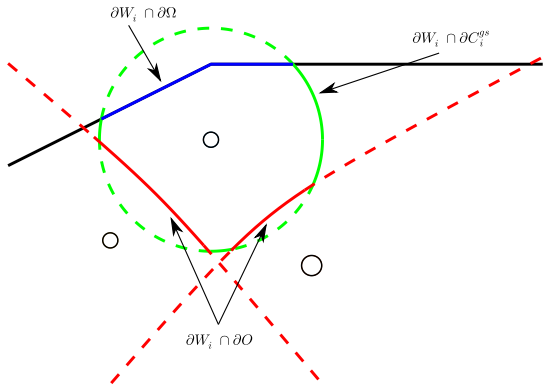

Fig. 3: $W_i \cap C_i^{gs}$ boundary decomposition.

Since the region Ω is unaffected by the motion of the agents, we get that the integral over $\partial W_i \cap \partial \Omega$ is 0. Additionally, since C_j^{gs} is independent of agent i, the integral over $\partial W_j \cap \partial C_j^{gs}$ is also 0, while agent i affects j only at its induced hyperbolic arc ∂H_{ji}, resulting in

$$\frac{\partial \mathscr{H}}{\partial q_i} = \int_{\partial W_i \cap \partial C_i^{gs}} f(z_i) u_i^i n_i \phi dq + \int_{\partial W_i \cap \partial \mathbb{O}} f(z_i) u_i^i n_i \phi dq \sum_{j \in N_i} \int_{\partial W_j \cap \partial H_{ji}} f(z_j) u_j^i n_i \phi dq.$$

The Jacobian over $\partial W_i \cap \partial C_i^{gs}$ is equal to the unit matrix $\mathbb{I}_2$ since it is an arc of a circle with center q_i, while the integral over $\partial W_i \cap \partial \mathbb{O}$ can be split into a sum of integrals over hyperbolic arcs, resulting in the final expression (12).

By following a similar procedure with the only difference being $\frac{\partial f(z_i)}{\partial z_i} \neq 0$ and defining

$$v_j^i = \frac{\partial q}{\partial z_i}, \; q \in \partial (W_i \cap C_i^{gs}), \; i, j \in I_n,$$

we get expression (13) for the altitude control law. ■

A. Inter–Agent Collision Avoidance

Although the control law (12,13) guarantees monotonic increase of $\mathscr{H}$, it is not able to guarantee collision avoidance between the MAAs. Additionally, the control law may in some cases result in the overlapping of two or more positioning uncertainty regions. Although this may not always result in a risk of collision due to the agents possibly being at different altitudes, it may negatively impact their performance. Thus it is desired to design a control law extension for (12) that will prevent the agents' positioning uncertainty regions from overlapping. For this purpose, we shall define a critical distance between two agents, $d_{ij}^c = r_i + r_j + \varepsilon$, where ε is an infinitesimally small positive constant. When agent i moves towards node j, which happens when $u_{i,q}^T (q_j - q_i) \geq 0$, and their reported distance $\| q_j - q_i \|$ is smaller than the critical distance d_{ij}^c, the control input of agent i is set to zero in order to prevent the two agents from moving any closer. Once their distance has increased or the control input of i no longer leads it towards j, agent i is allowed to move again. Consequently each agent i implements

$$\tilde{u_{i,q}} = \begin{cases} 0, & \text{if } \exists j \in N_i \colon \| q_i - q_j \| \leq d_{ij}^c \wedge \\ & \quad u_{i,q}^T (q_j - q_i) \geq 0 \\ u_{i,q}, & \text{otherwise} \end{cases} \quad (15)$$

V. Simulation Studies

Two simulation studies are presented in order to evaluate the efficiency of the proposed control (12,13) with the extension (15). The region Ω was chosen to be the same as in [24] and space density function was chosen as $\phi(q) = 1, \; \forall q \in \Omega$, assigning the same importance to all points in Ω. For all agents, the altitude constraints were $z^{\min} = 0.3$ and $z^{\max} = 2.3$ while the half–angle of their sensors was $a = 20^\circ$.

A. Case Study I

In this case study, a team of 8 MAAs is simulated with each agent having a different measure of positioning uncertainty. The initial and final configurations of the agents are illustrated in Figures 4 (a) and 4 (b) respectively, with the positioning uncertainty regions and guaranteed sensed regions shown as black and red circles respectively, the boundaries of the agents' AWGV cells shown in blue and the boundary of the region Ω in black. Figure 5 depicts the MAA's trajectories, with red lines representing their trajectories in $3D$ space and blue lines representing the projections of their trajectories on Ω. The MAA's initial and final position are marked by blue squares and circles respectively. Figure 6 shows the evolution of the coverage–quality objective over time. As it was expected from the theory, the increase of $\mathscr{H}$ over time is monotonic.

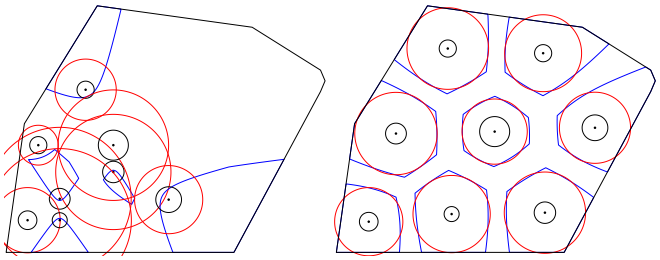

(a) (b)

Fig. 4: Case Study I: Initial (a) and final (b) agent configuration.

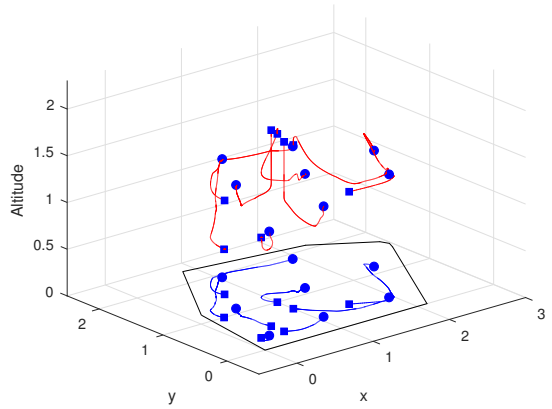

Fig. 5: Case Study I: Agent trajectories and their projections on Ω.

B. Case Study II

This case study highlights a property of the altitude control law. A total of 3 agents were used with their initial configuration shown in Figure 7 (a) and their final configuration in Figure 7 (b). The positioning uncertainty regions and guaranteed sensed regions are shown as black and red circles respectively, the boundaries of the agents'

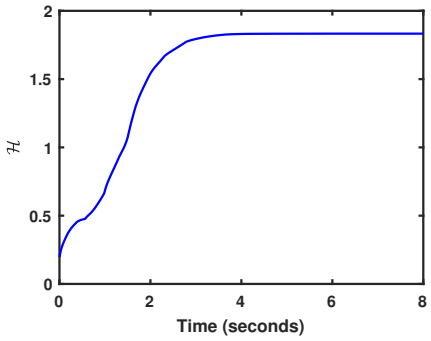

Fig. 6: Case Study I: Evolution of the coverage–quality objective $\mathscr{H}$ over time.

AWGV cells are shown in blue and the boundary of the region Ω in black. Figure 8 depicts the MAA's trajectories, with red lines representing their trajectories in $3D$ space and blue lines representing the projections of their trajectories on Ω. The MAA's initial and final position are marked by blue squares and circles respectively. It is observed that at their final configuration the MAAs' guaranteed sensed regions are completely contained within their respective AWGV cells. This indicates that they have all converged to their respective optimal altitudes z_i^{opt}. The optimal altitude is defined as the altitude that results in

$$\int_{\partial C_i^{gs}} tan(a) f(z_i^{opt}) dq + \int_{C_i^{gs}} \frac{\partial f(z_i)}{\partial z_i}\bigg|_{z_i^{opt}} dq = 0$$

$$2\pi R_i^{gs} tan(a) f(z_i^{opt}) + \pi (R_i^{gs})^2 \frac{\partial f(z_i)}{\partial z_i}\bigg|_{z_i^{opt}} = 0.$$

This is the altitude agent i converges at when it is possible for its whole guaranteed sensed region to be within its AWGV cell. The optimal altitude is dependent on the altitude constraints $z^{\min}$ and $z^{\max}$, the agent's measure of positioning uncertainty r_i as well as its sensor view angle a and is in general different among MAAs. The evolution of the coverage–quality objective $\mathscr{H}$ over time is depicted in Figure 9, where its monotonic increase is observed once again.

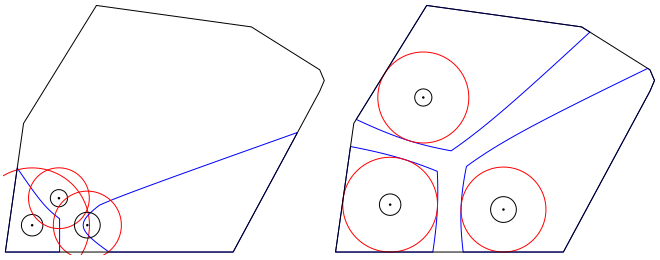

(a) (b)

Fig. 7: Case Study III: Initial (a) and final (b) agent configuration.

VI. Conclusions

The article deals with the problem of area coverage by a team of MAAs with imprecise localization with regards

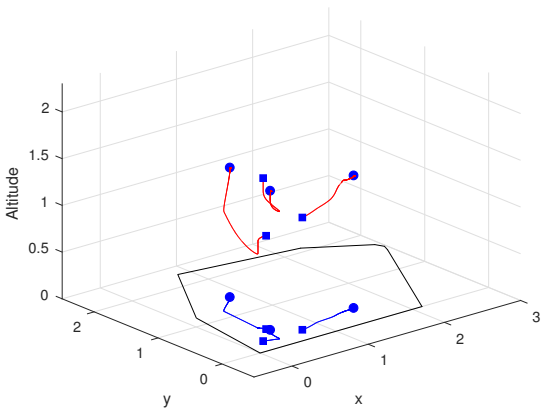

Fig. 8: Case Study III: Agent trajectories and their projections on Ω.

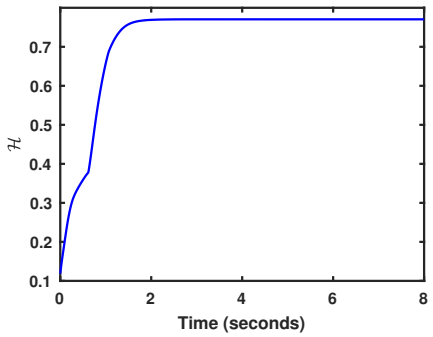

Fig. 9: Case Study III: Evolution of the coverage–quality objective $\mathscr{H}$ over time.

to their footprints on the ground. A gradient–based control scheme was designed, guaranteeing monotonic increase of a joint coverage–quality objective, while an extension was proposed in order to avoid possible collisions among the agents. Finally, simulation studies were conducted for the evaluation of the designed control law.

REFERENCES

[1] Y. Wang, E. Garcia, D. Casbeer, and F. Zhang, *Cooperative control of multi-agent systems: Theory and applications*. John Wiley & Sons, 2017.

[2] P. Dasgupta, "Multi-agent coordination techniques for multi-robot task allocation and multi-robot area coverage," in *Collaboration technologies and systems (cts), 2012 international conference on*. IEEE, 2012, pp. 75–75.

[3] V. Ramaswamy and J. R. Marden, "A sensor coverage game with improved efficiency guarantees," in *American Control Conference (ACC), 2016*. IEEE, 2016, pp. 6399–6404.

[4] J. Cortes, S. Martinez, and F. Bullo, "Spatially-distributed coverage optimization and control with limited-range interactions," *ESAIM: Control, Optimisation and Calculus of Variations*, vol. 11, no. 4, pp. 691–719, 2005.

[5] M. T. Nguyen, L. Rodrigues, C. S. Maniu, and S. Olaru, "Discretized optimal control approach for dynamic multi-agent decentralized coverage," in *Intelligent Control (ISIC), 2016 IEEE International Symposium on*. IEEE, 2016, pp. 1–6.

[6] X. Jing, C. Fei, and X. Linying, "Event-triggered coverage control for continuous-time multi-agent systems," in *Control Conference (CCC), 2015 34th Chinese*. IEEE, 2015, pp. 1303–1308.

[7] M. T. Nguyen and C. S. Maniu, "Voronoi based decentralized coverage problem: From optimal control to model predictive control," in *Control and Automation (MED), 2016 24th Mediterranean Conference on*. IEEE, 2016, pp. 1307–1312.

[8] Y. Stergiopoulos, M. Thanou, and A. Tzes, "Distributed collaborative coverage-control schemes for non-convex domains," *IEEE Transactions on Automatic Control*, vol. 60, no. 9, pp. 2422–2427, 2015.

[9] R. J. Alitappeh, K. Jeddisaravi, and F. G. Guimarães, "Multi-objective multi-robot deployment in a dynamic environment," *Soft Computing*, vol. 21, no. 21, pp. 6481–6497, 2017.

[10] P. Frasca, R. Carli, and F. Bullo, "Multiagent coverage algorithms with gossip communication: control systems on the space of partitions," in *American Control Conference, 2009. ACC'09.* IEEE, 2009, pp. 2228–2235.

[11] S.-i. Azuma, Y. Tanaka, and T. Sugie, "Multi-agent consensus under a communication–broadcast mixed environment," *International Journal of Control*, vol. 87, no. 6, pp. 1103–1116, 2014.

[12] Y. Stergiopoulos and A. Tzes, "Convex voronoi-inspired space partitioning for heterogeneous networks: A coverage-oriented approach," *IET control theory & applications*, vol. 4, no. 12, pp. 2802–2812, 2010.

[13] L. C. Pimenta, V. Kumar, R. C. Mesquita, and G. A. Pereira, "Sensing and coverage for a network of heterogeneous robots," in *Decision and Control, 2008. CDC 2008. 47th IEEE Conference on*. IEEE, 2008, pp. 3947–3952.

[14] Y. Stergiopoulos and A. Tzes, "Cooperative positioning/orientation control of mobile heterogeneous anisotropic sensor networks for area coverage," in *Robotics and Automation (ICRA), 2014 IEEE International Conference on*. IEEE, 2014, pp. 1106–1111.

[15] F. Sharifi, A. Chamseddine, H. Mahboubi, Y. Zhang, and A. G. Aghdam, "A distributed deployment strategy for a network of cooperative autonomous vehicles," *IEEE transactions on control systems technology*, vol. 23, no. 2, pp. 737–745, 2015.

[16] Y. Jin, Y. Wu, and N. Fan, "Research on distributed cooperative control of swarm uavs for persistent coverage," in *Control Conference (CCC), 2014 33rd Chinese*. IEEE, 2014, pp. 1162–1167.

[17] O. Arslan and D. E. Koditschek, "Voronoi-based coverage control of heterogeneous disk-shaped robots," in *2016 IEEE International Conference on Robotics and Automation (ICRA)*. Stockholm, Sweden: IEEE, 2016, pp. 4259–4266.

[18] J. A. Hage, M. E. E. Najjar, and D. Pomorski, "Fault tolerant collaborative localization for multi-robot system," in *Proceedings 24th Mediterranean Conference on Control and Automation (MED)*, Athens, Greece, Jun. 2016, pp. 907–913.

[19] J. Habibi, H. Mahboubi, and A. G. Aghdam, "Distributed coverage control of mobile sensor networks subject to measurement error," *IEEE Transactions on Automatic Control*, vol. 61, no. 11, pp. 3330–3343, Nov. 2016.

[20] B. Davis, I. Karamouzas, and S. J. Guy, "C-OPT: Coverage-aware trajectory optimization under uncertainty," *IEEE Robotics and Automation Letters*, vol. 1, no. 2, pp. 1020–1027, Jul. 2016.

[21] S. Papatheodorou, Y. Stergiopoulos, and A. Tzes, "Distributed area coverage control with imprecise robot localization," in *24th Mediterranean Conference on Control and Automation (MED)*, Athens, Greece, June 2016, pp. 214–219.

[22] K. Alexis, G. Nikolakopoulos, and A. Tzes, "Switching model predictive attitude control for a quadrotor helicopter subject to atmospheric disturbances," *Control Engineering Practice*, vol. 19, no. 10, pp. 1195–1207, 2011.

[23] W. Evans and J. Sember, "Guaranteed Voronoi diagrams of uncertain sites," in *20th Canadian Conference on Computational Geometry*, Montreal, Canada, 2008, pp. 207–210.

[24] S. Papatheodorou, A. Tzes, and Y. Stergiopoulos, "Collaborative visual area coverage," *Robotics and Autonomous Systems*, vol. 92, pp. 126 – 138, 2017.